



## Assessment of Magnetic Properties of Nanostructured Silicon Loaded with Superparamagnetic Iron Oxide Nanoparticles

P. Granitzer,<sup>a,\*</sup> K. Rumpf,<sup>a,\*</sup> J. Coffer,<sup>b</sup> P. Poelt,<sup>c</sup> and M. Reissner<sup>d</sup>

<sup>a</sup>Institute of Physics, Karl-Franzens-University Graz, A-8010 Graz, Austria

<sup>b</sup>Department of Chemistry, Texas Christian University, Fort Worth, Texas 76129, USA

<sup>c</sup>Institute for Electron Microscopy, University of Technology Graz, A-8010 Graz, Austria

<sup>d</sup>Institute of Solid State Physics, Vienna University of Technology, A-1040 Vienna, Austria

The aim of this work is to create a biocompatible superparamagnetic nanocomposite applicable as vehicle for magnetically guided drug delivery. Both materials, the nanostructured silicon as well as the iron oxide nanoparticles offer low toxicity. Therefore Fe<sub>3</sub>O<sub>4</sub>-nanoparticles have been incorporated within nanostructured silicon. The iron oxide nanoparticles have been synthesized in solution and then were either filled in or chemically grown within the pores. The magnetic properties of the system have been optimized concerning the blocking temperature  $T_B$  and the magnetic moment  $M$ , which are conflicting parameters. A particle size/distance and template dependent assessment of the magnetic properties of the nanocomposite will be presented. Although the growth of iron oxide particles within the porous template is not easy to control, the blocking temperature of the composite could be achieved far below room temperature.

© The Author(s) 2015. Published by ECS. This is an open access article distributed under the terms of the Creative Commons Attribution Non-Commercial No Derivatives 4.0 License (CC BY-NC-ND, <http://creativecommons.org/licenses/by-nc-nd/4.0/>), which permits non-commercial reuse, distribution, and reproduction in any medium, provided the original work is not changed in any way and is properly cited. For permission for commercial reuse, please email: [oa@electrochem.org](mailto:oa@electrochem.org). [DOI: 10.1149/2.0231505jss] All rights reserved.

Manuscript submitted February 4, 2015; revised manuscript received March 16, 2015. Published March 24, 2015. This was Paper 2306 presented at the Cancun, Mexico, Meeting of the Society, October 5–9, 2014.

Nanostructured silicon is versatile in its applicability due to the possibility to modify the structure size in a broad range between a few nanometers and a few tens of micrometers. Since porous silicon has been shown to be biodegradable and biocompatible<sup>1</sup> numerous scientists use this material within this realm. Furthermore it is crucial to point out that the dissolution of porous silicon in body fluid strongly depends on its porosity.<sup>2</sup>

In many works, molecules DNA or anti-cancer agents are attached to the pore-walls of porous silicon microparticles to bring these carriers to specific regions within the body.<sup>3</sup> Another key topic is biosensors which are mainly based on optical detection. Due to the fact that the refractive index of porous silicon is tunable by the anodization conditions, layered porous structures with varying refractive index can be fabricated which provides the possibility to trap molecules with different sizes.<sup>4</sup> The functionalization of drug-loaded porous silicon with fluorescent material allows to detect drug-release within the body or luminescent microporous silicon can be used for this purpose<sup>5</sup> which is an advantage compared to heavy-metal containing quantum dots being in general toxic. A further potential is the application of porous silicon in tissue engineering<sup>6</sup> since it has been found to support living cultures of mammalian tissue.<sup>7</sup>

Trapping of nanoparticles (e.g. Fe<sub>3</sub>O<sub>4</sub>) by oxidation of the porous silicon is realized by shrinking of the pore-diameters due to the oxidation of the pore walls and thus enclosing the particles within the pores. Surface modification of the porous silicon templates for example by oxidation can change the nature of porous silicon from hydrophobic or hydrophilic. SiO<sub>2</sub> offers a negative surface charge and thus coulomb forces can attract positive ions<sup>8</sup> which means that the nature of surface chemistry can affect the strength of attachment of a molecule to the porous silicon surface.

Due to the variability of the morphology pore-filling with various materials such as magnetic ones is also of interest. The fabrication of three-dimensional magnetic nanostructure arrays within a semi-conducting template could enable the integration in microtechnology exploiting e.g. the spin dependent electron transport. At the same time the filling of the pores with non-toxic iron oxide nanoparticles allows the utilization of the system for biomedical applications. It has been shown that porous silicon microparticles filled with superparamagnetic iron oxide nanoparticles can be used for enhanced magnetic

resonance contrast.<sup>9</sup> No cellular in vivo toxicity has been observed as well as the elimination of the material after 4 – 8 h in vivo.<sup>9</sup>

Magnetic nanoparticles, especially iron oxide have attracted attention for many years. Due to their non-toxic behavior they are utilized in various biomedical applications for diagnostics as well as therapeutics e.g. MR imaging<sup>10</sup> or drug carriers.<sup>11</sup>

The combination of porous silicon and iron oxide nanoparticles to form a vehicle for targeted drug delivery and their subsequent sustained release, thanks to the properties of the involved components, is a promising candidate for another biomedical application.

### Experimental

The porous silicon templates have been fabricated by anodization of a highly n-doped silicon wafer in a 10 wt% solution of hydrofluoric acid. The current density has been kept constant at 100 mAcm<sup>-2</sup> to achieve pores with an average diameter of 60 nm. The corresponding mean distance between the pores is 50 nm. In Figure 1 such a typical porous silicon sample is shown. Since the as-etched porous silicon offers an H-terminated surface and thus hydrophobic properties, all samples have been aged in air for several days to achieve a native oxide layer covering the pore-walls. To achieve porous silicon microparticles the porous layer has been removed mechanically from the silicon substrate and subsequently has been milled and filtered to achieve particles of about 2 μm.

Fe<sub>3</sub>O<sub>4</sub> nanoparticles have been fabricated by high temperature decomposition method after a common route<sup>12</sup> to produce monodisperse nanoparticles. All particles are coated with oleic acid to avoid agglomeration and for stabilization and they are dispersed in hexane solution. In this work particles of 4, 5, 8 and 10 nm have been investigated. The infiltration has been carried out by adding the particle solution dropwise on the porous silicon surface. To facilitate this process a magnetic field has been applied. The infiltration has been investigated with respect to the amount of particles within the solution.

A further approach to incorporate iron oxide within the pores of porous silicon templates is the growth of particles by electrodeposition. As electrolyte an iron nitrite solution (Fe(NO<sub>3</sub>)<sub>3</sub>) has been used and the deposition has been performed in galvanostatic mode with a constant current density of 10 mAcm<sup>-2</sup>.

For structural characterization of the samples scanning electron microscopy (SEM) has been employed as well as energy dispersive X-ray (EDX) spectroscopy and mapping to get a survey of the distribution of the different elements.

\*Electrochemical Society Active Member.

<sup>z</sup>E-mail: [petra.granitzer@uni-graz.at](mailto:petra.granitzer@uni-graz.at)

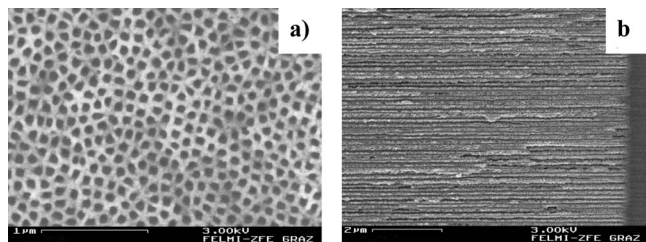


**Figure 1.** a) Top-view SEM image of a typical fabricated porous silicon sample showing the self-organized more or less regular pore arrangement. The average pore-diameter is 60 nm and the mean distance between the pores is 40 nm. b) Corresponding cross-sectional SEM image exhibiting the straight pores. The thickness of the porous layer is about 40  $\mu\text{m}$  (not fully shown here).

Magnetic measurements have been carried out with a superconducting quantum interference device (SQUID) and a vibrating sample magnetometer (VSM). The magnetic field has been varied between  $\pm 1$  T. A temperature range between 4 and 300 K has been used for the temperature dependent measurements.

### Discussion

The purpose of this work is to investigate a porous silicon/ $\text{Fe}_3\text{O}_4$  nanocomposite which could be used for magnetically guided drug delivery with respect to its magnetic properties. On the one hand the magnetic moment should be as high as possible which means a maximum loading of the pores. On the other hand the transition temperature

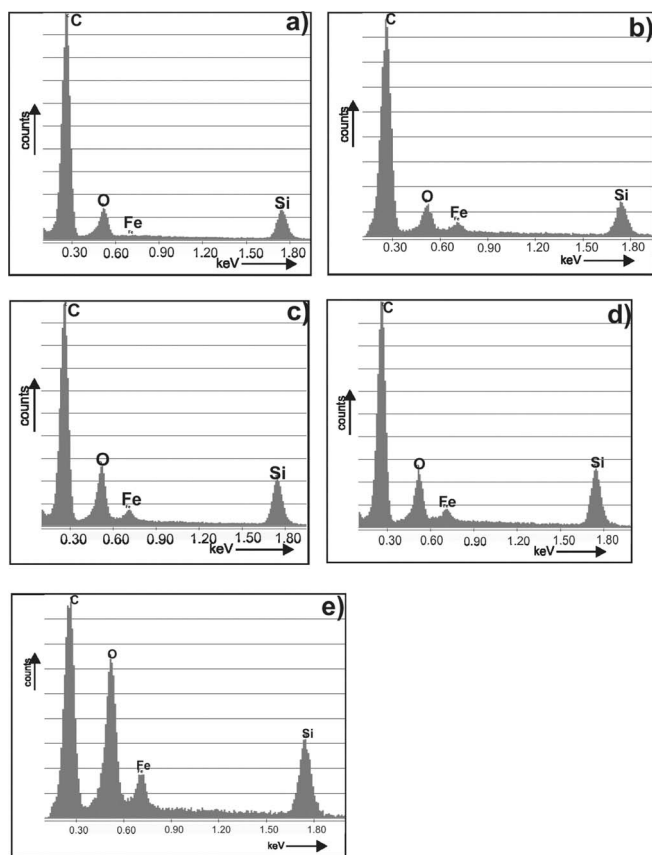


**Figure 2.** EDX-spectra taken at the pore-tip region of porous silicon samples with infiltrated  $\text{Fe}_3\text{O}_4$  nanoparticles of about 8 nm. The infiltration time was for all samples 20 min. The particle concentration has been varied (decreasing concentration from a to e). An increase of the iron content at the bottom of the pores with decreasing particle concentration can be seen from a) to e).

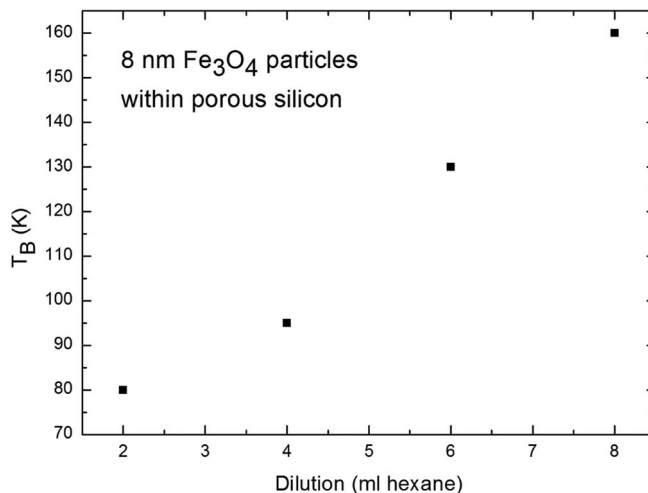


**Figure 3.**  $T_B$  gained from ZFC/FC measurements of 8 nm  $\text{Fe}_3\text{O}_4$  nanoparticles of different concentration infiltrated into porous silicon. The concentration of the particle solution has been decreased stepwise by half in diluting with hexane.

between superparamagnetic behavior and blocked state, the so-called blocking temperature, should be far below room temperature to guarantee that the specimens offer no remanence after switching off the magnetic field.

One advantage of porous silicon beside the required biocompatibility is the high surface area. Dependent on the pore-size and the thickness of the layer the surface area of mesoporous silicon is in the range of a few  $100 \text{ m}^2/\text{cm}^3$ . This allows an appropriate functionalization<sup>13</sup> with high efficiency and the subsequent loading with a high amount of drugs within one porous silicon microparticle. From this point of view porous silicon microparticles are adequate to be used for the purpose of a nanovehicle.

As-etched porous silicon offers a hydrophobic behavior due to the hydrogen termination of the surface and thus the samples are oxidized by aging in ambient air. Fourier transform infrared (FTIR)-spectroscopy gives evidence of the oxidation.<sup>14</sup> Si-H bands around  $2100 \text{ cm}^{-1}$  are present in the as-etched samples. The further occurring Si-OH modes around  $1635 \text{ cm}^{-1}$  disappear if the samples are oxidized and oxide bands around  $2250 \text{ cm}^{-1}$  appear.<sup>14</sup>

$\text{Fe}_3\text{O}_4$  nanoparticles of 8 nm in size have been infiltrated within the porous layer in dependence on the concentration of the particle solution and also on the particle size. The infiltration time has been 20 min. The small particles (4 and 5 nm) are loaded down to the pore-tips within this time frame, whereas, with increasing particle size, the filling of the pores decreases which means that the filling does not reach the bottom of the pores. A modification of the concentration of the particle solution (dilution with hexane) influences the infiltration process. An increase of the infiltration depth with decreasing concentration can be seen.

EDX spectra taken at the cross-section of the samples near the pore-tips show the dependence of the infiltration depth on the particle amount in the solution (Figure 2). The infiltration time has been the same for all these experiments. In enhancing the infiltration time, the pores could be also filled down to the tips in the case of the higher particle amount.

The infiltration of the particle solution is caused by capillary forces in the pores and it is influenced by the amount of particles in the solution. A further possibility to facilitate the filling is the application of a magnetic field ( $B \sim 1$  T) during the infiltration procedure.

Magnetic measurements have been performed as a function of particle size and the particle concentration (Figure 3). One key feature is the blocking temperature  $T_B$  of the systems which has been determined by zero field cooled/field cooled (ZFC/FC) measurements. First the samples have been cooled down to 4 K without magnetic field.

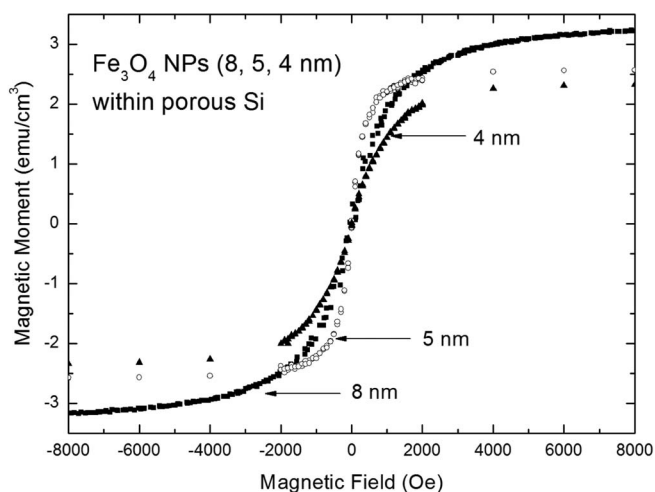


**Figure 4.** Hysteresis curves of porous silicon with infiltrated iron oxide nanoparticles of 4, 5 and 8 nm measured at 300 K.

Then a magnetic field of 500 Oe has been applied and the samples are warmed up to 300 K and subsequently cooled down to 4 K again. Systems filled with small particles of 4 or 5 nm show blocking temperatures of about 10 and 15 K, respectively. The minimum distance between the particles, of about 4 nm, determined by the shell in the case of closed packed filling, is sufficient to suppress dipolar coupling between the particles. Composites containing bigger particles of 8 and 10 nm in size offer blocking temperatures of about 160 and 170 K, respectively. The quite high values are due to occurring magnetic interactions. The individual particles offer a greater magnetic moment and thus the oleic acid shell of about 2 nm around each particle cannot avoid magnetic interactions which induce a higher blocking temperature in the case of dense pore-filling.  $T_B$  of smaller particles (4 and 5 nm) is around 10 and 15 K, respectively. This arises because of the smaller particle size, which do not interact magnetically among each other. The blocking temperature of chemically grown iron oxide within the pores is around 40 K which indicates that the deposited structures do not exhibit dipole coupling.

The temperature dependent measurements of all investigated samples show that there is no magnetic remanence above room temperature which is one precondition for biomedical applications. Field dependent magnetization measurements performed at  $T = 300$  K of particles of different sizes within porous silicon also show the non-existence of the remanence (Figure 4). Furthermore it can be seen that the magnetization decreases with decreasing particle size. Nevertheless all investigated samples offer a magnetization which is sufficiently high to move the nanocomposites with a magnet in water. For this verification a NdFeB magnet with a pole field strength of 1 T has been used. The samples have been easily moved in a water filled Petri dish of 100 mm in diameter and 25 mm in height, whereat the distance between sample and magnet has been between 10 and 20 mm.

Cytocompatibility measurements of porous silicon and of iron oxide nanoparticles has been presented by various authors<sup>3,8,15,16</sup> in different works. The cytocompatibility of porous silicon/Fe<sub>3</sub>O<sub>4</sub>

composites containing different particle sizes has been investigated recently, whereas a cell viability higher than 90% has been found.<sup>17</sup>

## Conclusions

The presented nanocomposite system consisting of a porous silicon template and infiltrated Fe<sub>3</sub>O<sub>4</sub> nanoparticles has been investigated as a function of the magnetic preconditions required for biomedical applications. Investigations have been performed in dependence on the particle size (4, 5, 8, 10 nm) as well as on the concentration of the nanoparticle solution. The infiltration process has been elucidated and optimized to achieve as high as possible particle loading within the pores. In the case of bigger particles (8, 10 nm) the particle solution has to be diluted to facilitate the loading process. A further possibility to improve the filling fraction of the pores is the application of a magnetic field to support the capillary forces. The magnetic characterization of all samples show that there is no magnetic remanence at room temperature, the blocking temperature is far below 200 K. The magnetization decreases with decreasing the particle size, however in all cases it is still sufficient high to move the samples in water in a Petri dish. All investigations show so far that the system is appropriate to be used in biomedical applications and thus could be promising for magnetically guided drug delivery.

## Acknowledgments

The authors thank Dr. M. P. Morales from the CSIC Madrid for the supply with iron oxide nanoparticles.

## References

1. L. T. Canham, *Adv. Mater.*, **7**, 1033 (1995).
2. E. Pastor, E. Matveeva, V. Parkhutik, J. Curiel-Esparza, and M. C. Millan, *Phys. Status Solidi C*, **4**, 2136 (2007).
3. H. A. Santos, Porous silicon for biomedical applications, Woodhead Publishing Series in Biomaterials: Number 68 (2014).
4. C. Pacholski, M. Sartor, M. J. Sailor, F. Cunin, and G. M. Miskelly, *J. Am. Chem. Soc.*, **127**, 11636 (2005).
5. J. H. Park, L. Gu, G. Maltzahn, E. Ruoslahti, S. N. Bhatia, and M. J. Sailor, *Nat. Mater.*, **8**, 331 (2009).
6. M. A. Whitehead, D. Fan, P. Mukherjee, G. R. Akkaraju, L. T. Canham, and J. L. Coffey, *Tissue Eng. A*, **14**, 195 (2008).
7. L. D. Buckberry and S. C. Bayliss, *Mater. World*, **7**, 213 (1999).
8. E. J. Anglin, L. Cheng, W. R. Freeman, and M. J. Sailor, *Adv. Drug Deliv. Rev.*, **60**, 1266 (2008).
9. J. M. Kinsella, S. Ananda, J. S. Andrew, J. F. Grondek, M.-P. Chien, M. Scadeng, N. C. Gianneschi, E. Ruoslahti, and M. J. Sailor, *Adv. Mater.*, **23**, H248 (2011).
10. X. Zhao, H. Zhao, Z. Chen, and M. Lan, *J. Nanosci. Nanotechnol.*, **14**, 210 (2014).
11. S. Laurent, A. A. Saei, S. Behzadi, A. Panahifer, and M. Mahmoudi, *Expert Opin. Drug Deliv.*, **11**, 1449 (2014).
12. S. Sun, H. Zeng, D. B. Robinson, S. Raoux, Ph. M. Rice, S. X. Wang, and G. Li, *J. Am. Chem. Soc.*, **126**, 273 (2004).
13. E. Secret, K. Smith, V. Dubljevic, E. Moore, P. Macardle, B. Belalet, M.-L. Rogers, T. G. Johns, J.-O. Durand, F. Cunin, and N. H. Voelcker, *Adv. Healthcare Mater.*, **2**, 626 (2013).
14. P. Granitzer, K. Rumpf, P. Pölt, M. Albu, and B. Cherev, *Phys. Stat Sol C*, **6**, 2222 (2009).
15. D. Ling and T. Hyeon, *Small*, **9**, 1450 (2013).
16. A. Hanini, A. Schmitt, K. Kacem, F. Chau, S. Ammar, and J. Gavard, *Int. J. Nanomedicine*, **6**, 787 (2011).
17. P. Granitzer, K. Rumpf, Y. Tian, G. Akkaraju, J. Coffey, P. Poelt, and M. Reissner, *Appl. Phys. Lett.*, **102**, 193110 (2013).